22 October 1998

PHYSICS LETTERS B

ELSEVIER

Physics Letters B 438 (1998) 430–440

Study of ϕ and $f_2'(1525)$ meson production in $\bar{p}p$ annihilation at rest

OBELIX Collaboration

A. Alberico [a], A. Bertin [a], M. Bruschi [a], M. Capponi [a], S. De Castro [a], R. Donà [a], A. Ferretti [a], D. Galli [a], B. Giacobbe [a], U. Marconi [a], M. Piccinini [a], N. Semprini Cesari [a], R. Spighi [a], V. Vagnoni [a], S. Vecchi [a], F. Vigotti [a], M. Villa [a], A. Vitale [a], A. Zoccoli [a], R. Bianconi [b], M. Corradini [b], E. Lodi Rizzini [b], L. Venturelli [b], A. Zenoni [b], C. Cicalò [c], A. Masoni [c], S. Mauro [c], G. Puddu [c], S. Serci [c], P. Temnikov [c,1], G. Usai [c], O.E. Gorchakov [d], V.P. Nomokonov [d], S.N. Prakhov [d], A.M. Rozhdestvensky [d], M.G. Sapozhnikov [d], V.I. Tretyak [d], M. Poli [e], P. Gianotti [f], C. Guaraldo [f], A. Lanaro [f], V. Lucherini [f], F. Nichitiu [f,2], C. Petrascu [f,2], A. Rosca [f,2], V.G. Ableev [g,3], C. Cavion [g], U. Gastaldi [g], M. Lombardi [g], G. Maron [g], L. Vannucci [g], G. Vedovato [g], G. Bendiscioli [h], V. Filippini [h], A. Fontana [h], P. Montagna [h], A. Rotondi [h], P. Salvini [h], C. Scoglio [h], F. Balestra [i], M.P. Bussa [i], L. Busso [i], P. Cerello [i], O.Yu. Denisov [i,3], L. Fava [i], L. Ferrero [i], R. Garfagnini [i], A. Grasso [i], A. Maggiora [i], A. Panzarasa [i], D. Panzieri [i], F. Tosello [i], L. Valacca [i], E. Botta [j], T. Bressani [j], D. Calvo [j], S. Costa [j], D. D'Isep [j], A. Feliciello [j], A. Filippi [j], S. Marcello [j], N. Mirfakhrai [j,4], M. Agnello [k], F. Iazzi [k], B. Minetti [k], G. Pauli [l], S. Tessaro [l], L. Santi [m]

[a] *Dipartimento di Fisica, Università di Bologna and INFN, Sez. di Bologna, Bologna, Italy*
[b] *Dipartimento di Chimica e Fisica per i Materiali, Università di Brescia and INFN, Sez. di Pavia, Italy*
[c] *Dipartimento di Scienze Fisiche, Università di Cagliari and INFN, Sez. di Cagliari, Cagliari, Italy*
[d] *Joint Institute for Nuclear Research, Dubna, Russia*
[e] *Dipartimento di Energetica, Università di Firenze and INFN, Sez. di Bologna, Bologna, Italy*
[f] *Laboratori Nazionali di Frascati dell'INFN, Frascati, Italy*
[g] *Laboratori Nazionali di Legnaro dell'INFN, Legnaro, Italy*
[h] *Dipartimento di Fisica Nucleare e Teorica, Università di Pavia and INFN, Sez. di Pavia, Pavia, Italy*
[i] *Dipartimento di Fisica A. Avogadro, Università di Torino and INFN, Sez. di Torino, Torino, Italy*
[j] *Dipartimento di Fisica Sperimentale, Università di Torino and INFN, Sez. di Torino, Torino, Italy*
[k] *Dipartimento di Fisica, Politecnico di Torino and INFN, Sez. di Torino, Torino, Italy*
[l] *Dipartimento di Fisica, Università di Trieste and INFN, Sez. di Trieste, Trieste, Italy*
[m] *Dipartimento di Fisica, Università di Udine and INFN, Sez. di Trieste, Italy*

Received 24 August 1998
Editor: L. Montanet

PII: S0370-2693(98)01160-5

Abstract

The reaction $\bar{p}p \to K^+K^-\pi^0$ was analysed for antiproton annihilations at rest at three hydrogen target densities. A strong dependence of the $\bar{p}p \to \phi\pi^0$ yield on the quantum numbers of the initial state is observed. The branching ratio of the $\phi\pi^0$ channel from the $^3S_1$ initial state is more than 15 times larger than the one from the $^1P_1$ state. A large apparent violation of the OZI rule for tensor meson production from $\bar{p}p$-annihilations from the P-waves $(1^{++}+2^{++})$ is observed: $R_{\rm exp}(f_2'\pi^0/f_2\pi^0) = (149 \pm 20)\cdot 10^{-3}$, significantly exceeding the OZI-rule prediction $R = 16\cdot 10^{-3}$.

1. Introduction

In recent experiments with stopped antiprotons at LEAR (CERN) [1–4] a large violation of the Okubo-Zweig-Iizuka (OZI) rule [5] in ϕ meson production was discovered. In some annihilation channels ($\bar{p}p \to \phi\pi, \phi\gamma$) the ϕ production exceeds the prediction of the OZI rule by a factor of 30-50. It is remarkable however that the level of the OZI rule violation turned out to be rather different in various annihilation reactions and that in some final states ($\phi\eta, \phi\omega$) no discrepancy with the OZI rule prediction was found.

Another interesting effect was observed firstly by the ASTERIX collaboration [1] in the $\phi\pi^0$ channel and confirmed by the OBELIX Collaboration [6]. This reaction is allowed from two $\bar{p}p$ initial states, $^3S_1$ and $^1P_1$ because of C-parity conservation, but no contribution to ϕ meson production from the $^1P_1$ state was observed.

We have collected data, with stopped antiprotons, of the

$$\bar{p}p \to K^+K^-\pi^0 \qquad (1)$$

annihilation reaction at three different target densities: liquid hydrogen (LH_2), gaseous hydrogen at normal temperature and pressure (NTP) and gaseous hydrogen at low pressure (LP) of 5 mbar. These three data sets permit the study of the reaction from different mixtures of $\bar{p}p$ initial states, from dominant S-waves in liquid to dominant P-waves at low pressure.

The analysis of the $K^+K^-\pi^0$ final state is complex, since all J^{PC} initial states but the 0^{++} one can contribute, and both $I = 0,1$ isospin states can be present with interfering amplitudes (see Table 1). Because of this complexity, our spin-parity analysis gives a set of best fit solutions, that we list in the following (see Table 2). Nevertheless, a clean test of the OZI rule in the $\bar{p}p \to K^+K^-\pi^0$ annihilation is already possible with the present analysis, because the ϕ peak is directly and clearly visible and some quantitative results can be extracted which are common to all our best fit solutions.

The measurements for reaction (1) in liquid and 5-mbar hydrogen target are reported for the first time. Moreover, our whole statistics in gas is higher than in the previous measurement [6].

2. Experimental layout and data samples

The experiment was performed at the Low Energy Antiproton Ring (LEAR) at CERN with the OBELIX spectrometer [8]. The OBELIX apparatus consisted of four subdetectors positioned around the axis of the Open Axial Field Magnet, whose magnetic field reached the maximum value 0.6 T along the beam axis. The subdetectors important for the discussion below are the Time-Of-Flight system (TOF) and the big Jet Drift Chamber (JDC). The TOF is composed of two scintillator barrels, placed at a distance of 130 cm and coaxial to the beam. It is also used to trigger on multiplicity and topology of charged particles

[1] On leave of absence from Institute for Nuclear Research and Nuclear Energy, Sofia, Bulgaria.

[2] On leave of absence from Department of High Energy Physics, Institute of Atomic Physics, Bucharest, Romania.

[3] On leave of absence from Joint Institute for Nuclear Research, Dubna, Moscow, Russia.

[4] On leave of absence from Sahid Beheshty University, Teheran, Iran.

Table 1
Intermediate states (see PDG [7]) allowed in the $\bar{p}p \to K^+K^-\pi^0$ annihilation channel; L is the relative angular momentum between the isobar and spectator

Intermediate state	I	$0^{-+}(^1S_0)$	$1^{--}(^3S_1)$	$1^{+-}(^1P_1)$	$1^{++}(^3P_1)$	$2^{++}(^3P_2)$
$K^\pm K^{*\mp}$	0,1	$L=1$	$L=1$	$L=0,2$	$L=0,2$	$L=2$
$(K^\pm\pi^0)_S K^\mp$	0,1	$L=0$	-	-	$L=1$	-
$a_0(980,1450)\pi^0$	0	$L=0$	-	-	$L=1$	-
$a_2(1320)\pi^0$	0	$L=2$	-	-	$L=1$	$L=1$
$f_0(980,1370,1500)\pi^0$	1	$L=0$	-	-	$L=1$	-
$f_2(1270), f_2'(1525)\pi^0$	1	$L=2$	-	-	$L=1$	$L=1$
$f_{j=0}(1700)\pi^0$	1	$L=0$	-	-	$L=1$	-
$f_{j=2}(1700)\pi^0$	1	$L=2$	-	-	$L=1$	$L=1$
$\phi(1020), \rho(1450,1700)\pi^0$	1	-	$L=1$	$L=0$	-	-

produced in the annihilation. The JDC is placed between the two TOF barrels and is used to track particles and to identify them by dE/dX measurement. The $\bar{p}$ beam momentum was 200 MeV/c for the LH_2 run and 105 MeV/c for the NTP and LP runs to provide the optimal conditions for the beam stopping in the targets of different density [9].

The experimental data for each target density were collected with a multiplicity trigger that required the signal from the entering antiproton, 2 hits in the internal TOF barrel and 2 hits in the external one. The number of triggered events involved in the present analysis are 10.4 million in the LH_2, 6.7 million in the NTP and 9.4 million in the LP hydrogen target. They correspond to $116 \cdot 10^6$, $74.6 \cdot 10^6$ and $91.8 \cdot 10^6$ initial $\bar{p}p$ annihilations respectively.

Events with the presence of only two tracks (with different charge) in the JDC with length ≥ 20 cm

Table 2
The results for S- and P-wave fractions of $f_2'\pi^0$ annihilation frequency (in units of 10^{-4}) in LH_2 and LP (5 mbar) hydrogen depending on the set of the transition amplitudes used. The corresponding χ^2/NDF values are given as well; a notation like $f_2(1700)_P$ means that for this amplitude only the allowed P-wave states were included into the fit

Amplitude set	LH_2 χ^2/ndf	LH_2 $f_S(\bar{p}p \to f_2'\pi^0)$	LP χ^2/ndf	LP $f_P(\bar{p}p \to f_2'\pi^0)$
ISA: $\phi(1020), K^*(890), f_2(1270),$ $a_2(1320), f_2'(1525), a_0(980), (K\pi)_S$	2.87	0.47 ± 0.08	1.74	15.0 ± 1.3
ISA + $f_2(1700)$	2.04	2.27 ± 0.36	1.10	21.4 ± 2.3
ISA + $f_0(1650)$	2.06	1.89 ± 0.21	1.32	6.9 ± 1.0
ISA + $f_0(1390,1500)$	1.81	1.59 ± 0.25	1.59	4.8 ± 1.9
ISA + $f_0(1390,1500,1650)$	1.52	1.76 ± 0.25	1.29	6.2 ± 1.6
ISA + $f_2(1700) + f_0(1500)$	1.48	3.59 ± 0.70	1.15	20.4 ± 2.6
ISA + $f_2(1700) + f_0(1390,1500)$	1.47	3.10 ± 0.64	1.14	22.0 ± 2.2
ISA + $f_2(1700) + f_0(1390,1500,1650)$	1.34	3.46 ± 0.63	1.07	18.2 ± 1.9
ISA + $f_2(1700) + f_0(1390,1500,1650)_S$	1.33	3.39 ± 0.70	1.10	22.4 ± 2.1
ISA + $f_2(1700) + \rho(1450,1700)$	1.53	2.58 ± 0.48	1.10	23.0 ± 2.3
ISA + $f_0(1390,1500) + \rho(1450,1700)$	1.21	2.69 ± 0.38	1.18	11.3 ± 1.2
ISA + $f_0(1390,1500,1650)$ $+ \rho(1450,1700)$	1.20	1.34 ± 0.21	1.16	12.4 ± 1.6
ISA + $f_2(1700) + f_0(1390,1500)$ $+ \rho(1450,1700)$	1.13	4.22 ± 0.82	1.04	20.2 ± 2.3
ISA + $f_2(1700)_P + f_0(1390,1500)_S$ $+ \rho(1450,1700)$	1.20	2.59 ± 0.63	1.09	22.9 ± 2.3
ISA + $f_2(1700) + f_0(1390,1500,1650)$ $+ \rho(1450,1700)$	1.11	2.26 ± 0.68	1.04	20.4 ± 2.0

were subjected to a 1C kinematic fit and those with a χ^2 value corresponding to a probability larger than 5% to satisfy the $\bar{p}p \to K^+K^-\pi^0$ hypothesis were retained. The identification of both particles as kaons was performed by dE/dX measurements or TOF identification in the case of ambiguity of the dE/dX selection cut. The events for which one track was identified as kaon by the TOF and the second track had no time-of-flight measurement (mainly due to the high probability of decay for slow kaons) were also accepted for further analysis.

The number of selected events for reaction (1) is 29441, 30358 and 36169 for the LH_2, NTP and LP data samples respectively. The corresponding $K^+K^-\pi^0$ Dalitz plots are shown in Fig. 1 (upper row). Two perpendicular bands from the $K^{*\pm}(892)$ decays are clearly seen for each experimental condition. Along the $K\bar{K}$ invariant mass direction (the diagonal) a strong signal from ϕ is seen. It becomes weaker in the low pressure data sample. One can see also K^+K^- bands in the region of the $f_2(1270)/a_2(1320)$ and $f_2'(1525)$ mesons. These bands are most prominent in the LP data.

The dominant background contamination surviving the kinematic fit is found to come from the annihilation channels

$$\bar{p}p \to \pi^+\pi^- X \tag{2}$$

(where X is a system of neutral pions) with two charged pions of momentum $p_\pi \geq 550$ MeV/c. It was verified by Monte Carlo simulation that these events are centered around the theoretical TOF line for pions of Fig. 2b). Hence, the curves for the dE/dX and TOF selection cuts for kaons of Fig. 2 were optimized for the best rejection of this pionic background without significant losses of the $K^+K^-\pi^0$ events. The percentages of the $\pi^+\pi^- X$ events extending below the theoretical TOF line for pions and invading the band chosen for kaon selection were estimated by the population of events

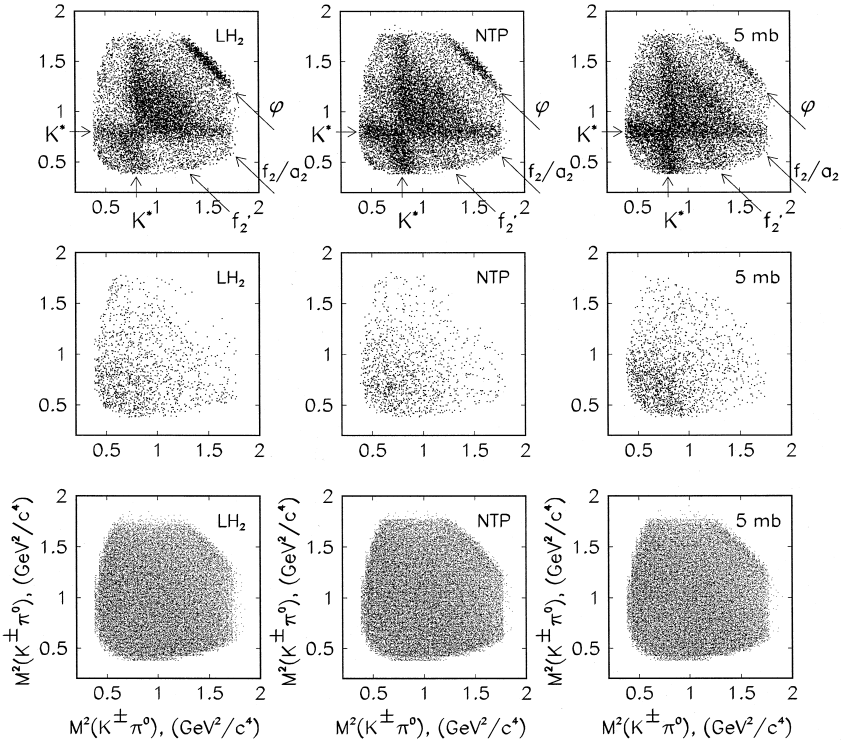

Fig. 1. Dalitz plots for reaction $\bar{p}p \to K^+K^-\pi^0$ at three different target densities (top). The distributions of events from the background reaction $\bar{p}p \to \pi^+\pi^- X$ are shown in the center. The Monte Carlo simulation of the acceptance for the reaction $\bar{p}p \to K^+K^-\pi^0$ is shown in the bottom.

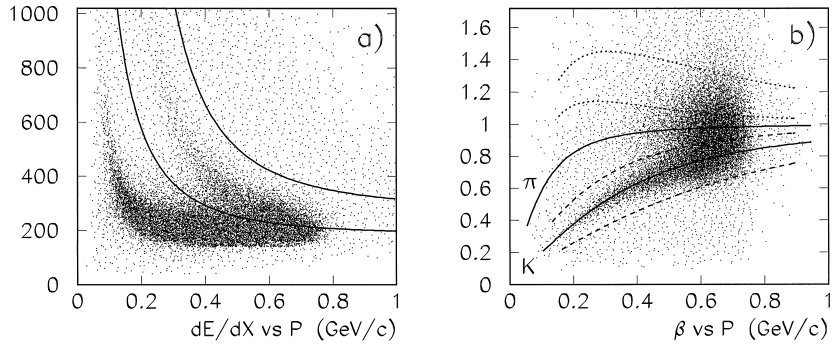

Fig. 2. (a) $\mathrm{d}E/\mathrm{d}X$ distribution for tracks of which satisfy the $\bar{p}p \to K^+K^-\pi^0$ kinematic hypothesis; (b) time-of-flight (TOF) β-distribution for tracks of events selected by kinematic fit and dE/dX; the solid curves are theoretical functions of TOF for pions and kaons, the dashed curves show the selection cuts for the final sample of $K^+K^-\pi^0$ events, the dotted curves show the selection cuts for the $\pi^+\pi^-X$ background sample.

above the pion line and are 2.6%, 2.2%, 2.7% for LH_2, NTP and LP data respectively.

The Dalitz plots with the background events of reaction (2) are shown in Fig. 1 (see middle row). These background Dalitz plots were subtracted from the $K^+K^-\pi^0$ ones during the fitting procedure.

Another source of contamination is due to events from the reactions

$$\bar{p}p \to K^{\pm}\pi^{\mp}K^0 \ (\ p_\pi \geq 550\,\mathrm{MeV}/c)\,, \qquad (3)$$

$$\bar{p}p \to K^+K^-\pi^0\pi^0\ . \qquad (4)$$

We simulated events for the reactions (3) and (4) applying the same cuts as for the events of the $K^+K^-\pi^0$ reaction. From the measured frequency of the $K^{\pm}\pi^{\mp}K^0$ reaction from [10–12] and assuming that the yield of the $K^+K^-\pi^0\pi^0$ reaction is at least two times smaller than that of the $K^+K^-\pi^0$ reaction, we estimated that the contamination from reaction (3) does not exceed 2% and that from reaction (4) is less than 1.5% for all $K^+K^-\pi^0$ data samples. The background events from reactions (3) and (4) were not subtracted and they affected the $K^+K^-\pi^0$ data samples subjected to the fit.

The acceptance Dalitz plots of the reaction (1) are shown in Fig. 1 (lower row) for each target condition. These Monte Carlo events were generated according to phase space, passed through the OBELIX apparatus simulation and reconstruction code and through the same selection cuts as the experimental data. The acceptance is affected by the threshold of the OBELIX apparatus for kaons with momenta below 200 MeV/c, which cannot reach the JDC because of the energy loss in the internal TOF barrel. This effect leads to a $3 \div 5\%$ loss of events in the experimental Dalitz plots.

3. Data analysis

In order to determine the yields of ϕ and f_2' mesons a spin-parity analysis of the reaction (1) was done. It was assumed that the $\bar{p}p$ system annihilates into $K^+K^-\pi^0$ through two-body intermediate states. The elementary transition amplitudes were parametrized in the framework of the isobar model [13], considering the states listed in Table 1. They have the form:

$$A_{J^{PC}}(\boldsymbol{p},\boldsymbol{q}) = \sum_{I,I_3} c_{I,I_3} Z_{J^{PC},I,I_3,L,l}(\boldsymbol{p},\boldsymbol{q}) \times W_L(p) W_l(q) F_{I,I_3,l}(\boldsymbol{q}), \qquad (5)$$

where $\boldsymbol{p}$ is the laboratory momentum of a resonance; $\boldsymbol{q}$ is the decay momentum in the resonance rest frame; I, I_3 are the $\bar{p}p$ isospin and its third component; c_{I,I_3} are the Clebsch-Gordan coefficients; $Z_{J^{PC},I,I_3,L,l}$ are the covariant spin tensors which give the angular dependence [14]; L is the isobar-spectator relative angular momentum; l is the spin of the isobar; the function F is the so-called Blatt-Weisskopf damping factor [15]; $F_{I,I_3,l}$ is the isobar production amplitude taken as a relativistic Breit-Wigner function. For the non-resonant $K\pi$ system in rela-

tive S-wave state, $(K\pi)_S$, the analytical parametrization of Törnqvist [16] was used. The total amplitude from a given J^{PC} state is

$$A^T(J^{PC}) = \sum_i w^i_{J^{PC}} A^i_{J^{PC}}(\boldsymbol{p},\boldsymbol{q}), \qquad (6)$$

where $w^i_{J^{PC}}$ are free complex parameters of the fit, which describe the contribution of an intermediate state i and $A^i_{J^{PC}}(\boldsymbol{p},\boldsymbol{q})$ is from Eq. (5). Each amplitude $A^i_{J^{PC}}(\boldsymbol{p},\boldsymbol{q})$ was normalized to unity using the $\bar{p}p \to K^+K^-\pi^0$ events generated following phase space (before apparatus distortion). The theoretical Dalitz plots were obtained by weighting events of the acceptance Dalitz plot with the corresponding squared amplitudes.

To reproduce the experimental resolution of the detector the theoretical Monte Carlo plots were filled using the reconstructed momenta of particles, while the amplitudes were calculated using the generated momenta of $K^+K^-\pi^0$ events. This approach with one Monte Carlo Dalitz plot for each amplitude does not give the possibility of varying the width and the mass of a resonance during the fit, but allows to obtain more reliable values for the resonance yields and improves the determination of their production rates from different $\bar{p}p$ initial states.

The χ^2 function subjected to the MINUIT [17] minimization program was defined as:

$$\chi^2 = \sum_i \frac{\left(N_i^{\mathrm{Exp}} - N_i^{\mathrm{BG}} - N_i^{\mathrm{Th}}\right)^2}{\sigma^2_{N_i^{\mathrm{Exp}}} + \sigma^2_{N_i^{\mathrm{BG}}} + \sigma^2_{N_i^{\mathrm{Th}}}}, \qquad (7)$$

where $N_i^{\mathrm{Exp}}, N_i^{\mathrm{BG}}$ and N_i^{Th} are the number of events in bin i of the experimental $K^+K^-\pi^0$, the background $\pi^+\pi^-X$ and the total theoretical Monte Carlo Dalitz plot respectively; $\sigma_{N_i^{\mathrm{Exp}}}, \sigma_{N_i^{\mathrm{BG}}}$ and $\sigma_{N_i^{\mathrm{Th}}}$ are the corresponding errors.

To decrease the statistical fluctuations, all Dalitz plots were folded around the first diagonal, considering only the case $M^2(K^\pm\pi^0) > M^2(K^\mp\pi^0)$. The histogram bin size is 45 MeV$^2/c^4$; the bins of the experimental Dalitz plot with fewer than 7 events were excluded from the χ^2 calculation. In this way, 408 bins of Dalitz plots for each data sample are left for the spin-parity analysis .

An initial set of amplitudes (ISA), containing only well-established states, includes $\phi(1020), K^*(890), f_2(1270), a_2(1320)$ and $f_2'(1525)$ mesons with the masses and widths fixed from the PDG [7]. Since we could not distinguish K^+K^- states which differ only by isospin, the $a_0(980)$ and $f_0(980)$ isobars were represented in the ISA set by one effective state, with the parameters of $a_0(980)$ ($M = 975$ MeV$/c^2$ and $\Gamma = 65$ MeV$/c^2$) obtained in a recent analysis of the $\bar{p}p \to K^\pm K^0\pi^\mp$ reaction [11]. It was checked that a small variation of the $a_0(980)$ mass and/or width values did not lead to significant change of the fit results. The $(K\pi)_S$ amplitude was also included in the ISA set.

To decrease the number of free parameters the fitting process was performed in several steps. Firstly, the LH_2 data were fitted assuming S-wave initial states only. Then, the LP data were fitted with the the S-wave amplitudes fixed at the values from the LH_2 fit and free P-wave parameters. Finally, the fit of the LH_2 data was repeated assuming the parameters of P-wave amplitudes obtained in step 2 and free S-wave amplitudes. This iteration procedure was repeated several times to reach the best description of the experimental data. Then the NTP data were fitted with the parameters found for S- and P-wave amplitudes, leaving free only the weights of the J^{PC} states.

The results of the fit with the ISA set are shown in Fig. 3 by dashed lines. This set provides a rather good description of the low $M(K^+K^-)$ mass region around the ϕ peak and correctly reproduces the $M(K^\pm\pi^0)$ invariant masses in the $K^*(890)$ region. However, the total fit quality is not good and the χ^2/NDF values are 2.87, 2.01 and 1.74 for the LH_2, NTP and LP data fit respectively. One can see that the description of the experimental LH_2 data is worse than that of the LP data. This could be due to a lack of 0^{++} contributions in the ISA set, as the scalar mesons could dominate in annihilations from the S-wave and be less important in the P-wave.

For further improvement of the experimental data description we add various amplitudes (see Tables 1 and 2) to the ISA set. For some resonances with not well-established parameters we slightly varied the mass and the width in order to test their influence on the fit and on the results. The best description of the data at 3 different target densities is obtained by adding the contributions from $f_2(1700), f_0(1370), f_0(1500), f_0(1700), \rho(1450)$ and $\rho(1700)$ states to the

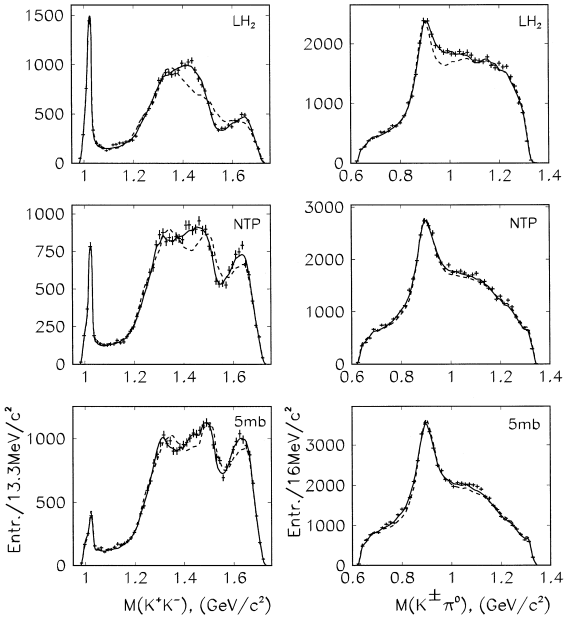

Fig. 3. $K^{\pm}\pi^0$ and K^+K^- invariant mass distributions for $\bar{p}p \to K^+K^-\pi^0$ annihilations in the H_2 target: liquid (top), gas at NTP (middle) and 5 mbar (bottom). The results of the best fit and the fit with the ISA set are shown by solid and dashed lines respectively.

ISA set. The following masses and widths of the isobars were used: $M = 1390$ MeV$/c^2$, $\Gamma = 340$ MeV$/c^2$ for $f_0(1370)$, $M = 1500$ MeV$/c^2$, $\Gamma = 120$ MeV$/c^2$ for $f_0(1500)$, $M = 1650$ MeV$/c^2$, $\Gamma = 175$ MeV$/c^2$ for $f_0(1700)$. For the $f_2(1700)$, $\rho(1450)$ and $\rho(1700)$ mesons the standard PDG parameters [7] were found to be good enough.

The results of the best fit are shown by solid lines in Fig. 3.

4. Results and discussions

The annihilation frequencies of the $\bar{p}p \to K^+K^-\pi^0$ channel and the $\bar{p}p \to \phi\pi^0$ reaction for each density of the hydrogen target are given in Table 3.

The annihilation frequency of the isobar A_i was defined as

$$f_{K^+K^-\pi^0}^{A_i} = \frac{1}{N_{\bar{p}}}\,\frac{N_{A_i}^{\mathrm{Exp}}}{\varepsilon_{A_i}} = \frac{1}{N_{\bar{p}}}\,\sum_{J^{PC}} |w_{J^{PC}}^i|^2\,\frac{N_{K^+K^-\pi^0}^{\mathrm{Exp}}}{\varepsilon_{K^+K^-\pi^0}}\,, \tag{8}$$

where $N_{\bar{p}}$ is the total number of antiproton annihilations, $N_{A_i}^{\mathrm{Exp}}$ is the number of detected events for the isobar A_i in the experimental Dalitz plot, ε_{A_i} is the corresponding detection efficiency for A_i, $N_{K^+K^-\pi^0}^{\mathrm{Exp}}$ is the number of events in the experimental Dalitz plot and $\varepsilon_{K^+K^-\pi^0}$ is the detection efficiency for the $\bar{p}p \to K^+K^-\pi^0$ events simulated following phase space. The parameter $|w_{J^{PC}}^i|^2$ is the weight obtained for the theoretical $|A_{J^{PC}}^i|^2$ Dalitz plot.

The total annihilation frequency of the $\bar{p}p \to K^+K^-\pi^0$ channel was defined as

$$f_{K^+K^-\pi^0} = \frac{1}{N_{\bar{p}}}\,\sum_{J^{PC}}\left|\sum_i w_{J^{PC}}^i\right|^2\,\frac{N_{K^+K^-\pi^0}^{\mathrm{Exp}}}{\varepsilon_{K^+K^-\pi^0}}\,. \tag{9}$$

Therefore, because of interferences between the resonances, the total annihilation frequency is not equal to the sum of the contributions (8) from all isobars.

The systematic uncertainty of the absolute annihilation frequency determination was estimated by measuring the yields of some known annihilation

Table 3
The $K^+K^-\pi^0$ and $\phi\pi^0$ annihilation frequencies (in units of 10^{-4}) for three densities of the hydrogen target. The last two rows of the table collect previous results on the same reaction. (LX) is the result obtained by ASTERIX with the *X*-ray trigger, that in principle selects pure *P*-wave atomic states [1]

$f \cdot 10^4$	LH_2	NTP	LP(5 mbar)
$f(\bar{p}p \to K^+K^-\pi^0)$	23.7 ± 1.6	30.3 ± 2.0	31.5 ± 2.2
$f(\bar{p}p \to \phi\pi^0)$	4.88 ± 0.32	2.47 ± 0.21	0.92 ± 0.10
$f(\bar{p}p \to \phi\pi^0, {}^1P_1)$			< 0.1 with 95%CL
$f(\bar{p}p \to \phi\pi^0)$	3.3 ± 1.5 [20]	1.9 ± 0.5 [1]	
previous measurements	5.5 ± 0.7 [21]	2.46 ± 0.23 [6]	0.3 ± 0.3 (LX) [1]

channels (such as $\bar{p}p \to \pi^+\pi^-$, $\bar{p}p \to K^+K^-$, $\bar{p}p \to \pi^+\pi^-\pi^0$) using data collected with the minimum bias trigger and with the multiplicity trigger used for the $K^+K^-\pi^0$ data. Comparing the obtained production rates it was found that the systematic uncertainty of the annihilation frequency determination does not exceed 8% for all three $K^+K^-\pi^0$ data samples. The $\phi\pi^0$ annihilation frequency values are rather stable and change only within 5% from the fit with the ISA set to the best one. The fit also shows that the $\phi\pi^0$ yield is only due to the $^3S_1$ amplitude contribution, since the weight of the $^1P_1$ amplitude contribution is around zero. For the evaluation of the upper limit on the $^1P_1$ contribution the LP data sample was used, where P-wave annihilation is dominant. The MINOS [17] procedure of the MINUIT code was used to obtain an estimate of the $^1P_1$ fraction. It turns out that $f^{^1P_1}(\phi\pi^0, \mathrm{LP}) < 0.1 \cdot 10^{-4}$ at the 95% confidence level (see tab. Table 3).

The annihilation frequency of channel f is defined as the product of the hadronic branching ratio Br by the fraction $F(J^{PC}, \rho)$ of annihilations of the protonium atom from all the levels with given J^{PC} at a given target density ρ [18]. The annihilation frequency of the $\phi\pi^0$ channel for the target of density ρ is then

$$f(\bar{p}p \to \phi\pi^0, \rho) = F\left(^3S_1, \rho\right) Br\left(\bar{p}p \to \phi\pi^0, ^3S_1\right) + F\left(^1P_1, \rho\right) Br\left(\bar{p}p \to \phi\pi^0, ^1P_1\right). \quad (10)$$

In order to extract hadronic branching ratios one has to know the annihilation fractions F for each target density ρ. Following the notation of Ref. [19], they are expressed as:

$$F\left(^3S_1, \rho\right) = \tfrac{3}{4} E\left(^3S_1, \rho\right) f_S(\rho), \quad (11)$$

$$F\left(^1P_1, \rho\right) = \tfrac{3}{12} E\left(^1P_1, \rho\right)\left(1 - f_S(\rho)\right), \quad (12)$$

where $f_S(\rho)$ is the fraction of annihilations from the S-states, the numbers $3/4$ and $3/12$ are the statistical weights of the corresponding initial states. $E(^3S_1, \rho)$ and $E(^1P_1, \rho)$ are the enhancement factors which reflect deviations from the pure statistical population of the levels.

The F values are not known precisely in a model independent approach. If one follows Ref. [19], where the $E(^3S_1)$ and $E(^1P_1)$ factors of Eqs. (11, 12) turn out to be very close to 1 at all densities and $f_S(\rho) = 0.87, 0.42, 0.20$ in liquid, gaseous NTP and 5 mbar low pressure targets, respectively, then

$$Br\left(\bar{p}p \to \phi\pi^0, ^3S_1\right) = (7.57 \pm 0.62) \cdot 10^{-4}, \quad (13)$$

$$Br\left(\bar{p}p \to \phi\pi^0, ^1P_1\right) < 0.5 \cdot 10^{-4}, 95\%\,\mathrm{CL}, \quad (14)$$

i.e. the branching ratio from the $^3S_1$ initial state is more than 15 times larger than the one from the $^1P_1$ state. This fact shows a strong dependence of the $\phi\pi^0$ production on quantum numbers of the initial $\bar{p}p$ state. The indication of this selection rule, reported earlier in Refs. [1,6], is now confirmed with considerably larger statistics: the experimental number of ϕ for our LP data sample is $N_\phi = 400 \pm 42$, while the ASTERIX collaboration had only $N_\phi = 4 \pm 4$ for the data sample under similar conditions [1].

The results of the previous measurements [1,6,20,21] of the $\phi\pi^0$ annihilation frequency are given in Table 3 as well. They are in agreement with our values for the LH_2 and NTP targets; in addition, the results for the 5-mbar hydrogen target are reported here for the first time.

To study the OZI-rule violation for tensor mesons the yield of the $f_2'(1525)$ meson, which is mainly an $\bar{s}s$ system, has to be compared to the yield of the $f_2(1270)$ meson, which consists of light quarks. In the $K^+K^-\pi^0$ Dalitz plots shown in Fig. 1 the band from the $f_2'(1525)$ meson is weak for annihilations in liquid hydrogen and becomes more prominent for annihilations in gaseous hydrogen. The yield of the $f_2'(1525)$ meson could depend on the interference with the near-by states. To give a feeling on the possible variation of the $f_2'(1525)\pi^0$ yield due to interference effects, in Table 2 we show the results of the fit for different amplitude sets. The χ^2 values shown in the same table reflect the degree of fit quality for each set of amplitudes used.

Looking through the values in Table 2 one can see that to get a good description of the LP data sample with $\chi^2/NDF \leq 1.1$ it is enough to add only the $f_2(1700)$ state to the ISA set. Including more resonances in the fit does not improve the χ^2 value for the LP data considerably and the $f_2'\pi^0$ yield from the P-wave remains rather stable and varies between $18 \cdot 10^{-4}$ and $23 \cdot 10^{-4}$ (all $f_2'\pi^0$ annihilation frequency values in Table 2 are corrected by $\mathrm{Br}(f_2' \to K^+K^-) = 0.444 \pm 0.016$ from [7]). If the

$f_2(1700)$ state is not included in the analysis, the yield of $f_2'\pi^0$ from the P-wave drops by a factor of two, but the description of the LP data becomes worse.

The comparison of the $f_2'\pi^0$ yields from the S and P-waves shows that the annihilation frequency of this state from the P-wave is higher by a factor of $4 \div 10$ irrespective of the set of amplitudes. For the best fit (last row of Table 2) the corresponding yields are:

$$f(\bar{p}p \to f_2'(1525)\pi^0) = (2.26 \pm 0.68) \cdot 10^{-4}, \mathrm{LH}_2, \text{S-wave}, \quad (15)$$

$$= (20.4 \pm 2.0) \cdot 10^{-4}, \mathrm{LP}, \text{P-wave}. \quad (16)$$

To determine the $\bar{p}p \to f_2(1270)\pi^0$ annihilation frequency the $\bar{p}p \to \pi^+\pi^-\pi^0$ annihilation channel was used. In the $K^+K^-\pi^0$ final state there is strong interference between the $f_2(1270)$ and $a_2(1320)$ states, whereas in the $\pi^+\pi^-\pi^0$ final state the $a_2(1320)$ contribution is absent. The relative S- and P-wave annihilation fractions for $f_2(1270)\pi^0 \to \pi^+\pi^-\pi^0$ were taken from the results of the spin-parity analysis of the $\bar{p}p \to \pi^+\pi^-\pi^0$ reaction, performed earlier by our collaboration [22]. In order to get the absolute values of S- and P-wave annihilation rates of the $f_2(1270)\pi^0$ state, the corresponding $\bar{p}p \to \pi^+\pi^-\pi^0$ annihilation frequencies were measured for each target condition using the data collected with the minimum bias trigger. The obtained $f(\bar{p}p \to \pi^+\pi^-\pi^0)$ frequencies are $(5.36 \pm 0.27)\%$, $(5.16 \pm 0.26)\%$ and $(4.89 \pm 0.28)\%$ for the LH_2, NTP and LP data respectively. These data can be compared to previous measurements $(6.9 \pm 0.4)\%$ (liquid [23]), $(5.82 \pm 0.43)\%$ (liquid [24]), $(5.20 \pm 0.35)\%$ (NTP gas [25]) and $(4.85 \pm 0.50)\%$ (X-ray trigger from P-wave [25]). Then the S- and P-wave contribution to the $f(\bar{p}p \to f_2\pi^0)$ annihilation frequencies (corrected by $\mathrm{Br}(f_2 \to \pi^+\pi^-) = 0.566 \pm 0.018$ from [7]) are

$$f(\bar{p}p \to f_2(1270)\pi^0) = (48.5 \pm 3.8) \cdot 10^{-4}, \mathrm{LH}_2, \text{S-wave}, \quad (17)$$

$$= (137.2 \pm 12.4) \cdot 10^{-4}, \mathrm{LP}, \text{P-wave}. \quad (18)$$

The present $K^+K^-\pi^0$ analysis gives somewhat comparable results for $f_2\pi^0$ (using $\mathrm{Br}(f_2 \to K^+K^-) = 0.023 \pm 0.003$ from [7]), though with significantly larger errors. For the best fit they are $(13 \pm 10) \cdot 10^{-4}$ and $(102 \pm 75) \cdot 10^{-4}$ for the S-wave f_2 production in the LH_2 annihilation data and for the P-wave f_2 production in the LP data respectively.

Using the $f_2'\pi^0$ yields from Eqs. (15, 16) and the $f_2\pi^0$ yields from Eqs. (17, 18) one obtains the ratios

$$R(f_2'(1525)\pi^0/f_2(1270)\pi^0) = (47 \pm 14) \cdot 10^{-3}, \text{S-wave}, \quad (19)$$

$$= (149 \pm 20) \cdot 10^{-3}, \text{P-wave}. \quad (20)$$

These experimental ratios have to be compared with the predictions of the OZI rule. For the quadratic Gell-Mann-Okubo mass formula the ratio $R(f_2'/f_2)$ is

$$R(f_2'/f_2) = 16 \cdot 10^{-3}. \quad (21)$$

For comparison with this prediction the experimental ratios should be corrected by the different phase space for $f_2'\pi^0$ and $f_2\pi^0$ final states: $R = R_{\mathrm{exp}}\, F$.

There are different ways to calculate the correction factor F. Simple two body phase space correction gives $F = 1.67^{(2L+1)}$, where L is the relative angular momentum between the resonance and π^0 meson. A more elaborate approach based on the Vandermeulen model of annihilation into two-body final states [26] gives $F = 1.08$. Therefore, after correction for phase space the value of R may only increase. Hence, the appreciable deviation (especially for P-wave annihilations) from the OZI rule prediction (21) cannot be attributed to the difference in the $f_2\pi^0$ and $f_2'\pi^0$ phase spaces.

A previous measurement of the $f_2'\pi^0/f_2\pi^0$ ratio, concerning only annihilations in liquid hydrogen target [27], is $R(f_2'\pi^0/f_2\pi^0) = (25.4 \pm 6.1) \cdot 10^{-3}$. This ratio was derived from the spin-parity analysis of the $\bar{p}p \to K_L^0K_L^0\pi^0$ annihilation channel with S-wave amplitudes alone, which were constructed in the K-matrix formalism. The fit of our LH_2 data with an amplitude set similar to the one used in Ref. [27] gives $R(f_2'\pi^0/f_2\pi^0) = (19.8 \pm 3.5) \cdot 10^{-3}$, which is in agreement with the reported value.

In addition, the $R(f_2'\pi^0/f_2\pi^0)$ ratio of production from the P-wave is reported here for the first time.

The anomalously high yield of the $\bar{p}p \to \phi\pi^0$ channel could be explained (see [28–30]) by the

rescattering diagrams with $K^*\bar{K}$ in the intermediate state $\bar{p}p \to K^*\bar{K} \to \phi\pi^0$. The calculations [28,30] provide reasonable agreement (within a factor two) with the experimental data on the $\phi\pi$ yield for annihilation from the S-wave. However, to explain the suppression of the $\phi\pi$ yield for annihilation from the P-wave, in this approach one should assume an unusually small frequency of the $K^*\bar{K}$ amplitude from the $^1P_1$ channel [29].

To verify this conclusion, one may consider the results of our spin-parity analysis concerning the annihilation frequencies of the $K^*\bar{K}$ final state at different target densities given in Table 4. The yields, corresponding to the best fit solution (last row of Table 2), show that the $^1P_1$ contribution to the $K^*\bar{K}$ annihilation frequency is comparable with the $^3S_1$ contribution and increase when the target density decreases: this dependence is opposite to that of the $\phi\pi$ yield which decreases with decreasing the target density. However, our fit is unable to distinguish between the isospin $I=0$ and $I=1$ components of the $K^*\bar{K}$ amplitude. Therefore, in principle, it may occur that the observed increase of the $K^*\bar{K}$ yield in the P-wave is due to the $I=0$ part of the amplitude, the $I=1$ $K^*\bar{K}$ state, allowed for rescattering into $\phi\pi^0$, being suppressed for some unknown reasons. The final answer to this question should be given by our coupled channels analysis of the $K^+K^-\pi^0$, $K^0K^\pm\pi^\mp$ and $\pi^+\pi^-\pi^0$ final states, which is now under way.

In any case, the rescattering mechanism is certainly not valid for the tensor meson production. In Ref. [31] the production of f_2' in the $\bar{p}p \to f_2'\pi^0$ reaction via the $K^*\bar{K}$ and $\rho\pi$ intermediate states was considered. The calculated production rates of f_2' from the S- and P- states are quite small, of the order of 10^{-6}. This is far from the experimental results, especially for P-wave annihilations, see Eq. (16). Therefore, the large apparent violation of the OZI rule observed for annihilation from the P-wave cannot be explained by the rescattering mechanism.

Abundant production of the ϕ meson from the S-wave annihilation was explained in Refs. [32,33] on the basis of an additional production of ϕ by diagrams that are allowed by the OZI rule if the nucleon wave function contains $\bar{s}s$ pairs. The intrinsic nucleon strangeness is assumed to be polarized as indicated by recent deep inelastic lepton-nucleon scattering experiments (for review of the experimental data see [34]). The polarization of the nucleon strangeness explains the strong dependence of the ϕ production on the initial state quantum numbers. As a test of the model, it was predicted in Ref. [32] that strong apparent violation of the OZI rule should be seen for the tensor meson production in annihilation from the P-wave. Our experimental results support this prediction.

Table 4
$K^*\bar{K}$ annihilation frequency (in units of 10^{-4}) at three densities of the hydrogen target

	LH_2	NTP	LP (5 mbar)
total	5.2 ± 0.9	7.0 ± 0.8	7.4 ± 0.9
from $^3S_1$	3.3 ± 0.8	1.7 ± 0.4	0.8 ± 0.2
from $^1P_1$	0.9 ± 0.2	3.4 ± 0.5	4.5 ± 0.7

In conclusion, the reaction $\bar{p}p \to K^+K^-\pi^0$ was analysed for antiprotons annihilation at rest at three hydrogen target densities. A strong dependence of the $\bar{p}p \to \phi\pi^0$ yield on the quantum numbers of the initial state is observed. The branching ratio of the $\phi\pi^0$ channel from the $^3S_1$ initial state is more than 15 times larger than the one from the $^1P_1$ state. A significant apparent violation of the OZI rule for tensor mesons in the P-wave $\bar{p}p$-annihilations, predicted in Ref. [32], is observed: $R_{\rm exp}(f_2'\pi^0/f_2\pi^0) = (149\pm20)\cdot10^{-3}$, significantly exceeding the $R = 16\cdot10^{-3}$ OZI-rule prediction.

Acknowledgements

The OBELIX collaboration thanks the technical staff of the LEAR machine group for their support during the runs.

We are grateful to J.Ellis and D.Kharzeev for valuable discussions.

References

[1] The Asterix Collaboration, J. Reifenröther et al., Phys. Lett. B 267 (1991) 299.
[2] The Crystal Barrel Collaboration, C. Amsler et al., Phys. Lett. B 346 (1995) 363.
[3] The Obelix Collaboration, V.G. Ableev et al., Phys. Lett. B 334 (1994) 237.

[4] The Obelix Collaboration, V.G. Ableev et al., Nucl. Phys. A 585 (1995) 577.
[5] S. Okubo, Phys. Lett. B 5 (1963) 165; G. Zweig, CERN Report No.8419/TH412, 1964; I. Iizuka, Prog. Theor. Phys. (Suppl. 37) 38 (1966) 21.
[6] The Obelix Collaboration, V.G. Ableev et al., Nucl. Phys. A 594 (1995) 375.
[7] Particle Data Group, Phys. Rev. D 54 (1996).
[8] The Obelix Collaboration, A. Adamo et al., Sov. J. Nucl. Phys. 55 (1992) 1732.
[9] The Obelix Collaboration, A. Bertin et al., Phys. Lett. B 386 (1996) 486.
[10] N. Barash et al., Phys. Rev. 139 (1965) B1659.
[11] G. Usai for the Obelix Collaboration, in: Proc. LEAP'96 Conference, Nucl. Phys. B (Proc. Suppl.) 56 (1997) 262, and Phys. Lett., in press.
[12] The Crystal Barrel Collaboration, C. Abele et al., Phys. Rev. D 57 (1998) 3860.
[13] D. Herndorn, P. Soding, R.J. Cashmore, Phys. Rev. D 11 (1975) 3165.
[14] V. Filippini, A. Fontana, A. Rotondi, Phys. Rev. D 51 (1995) 2241.
[15] J.M. Blatt, V. Weisskopf, Theoretical Nuclear Physics, Wiley, New York, 1952.
[16] N.A. Törnqvist, Z. Phys. C 68 (1995) 647.
[17] F. James, M. Roos, CERN program library, D 506 (1989).
[18] U. Gastaldi et al., Phys. Lett. B 320 (1994) 193.
[19] C.J. Batty, Nucl. Phys. A 601 (1996) 425.
[20] M. Chiba et al., Phys. Lett. B 202 (1988) 447.
[21] M.A. Faessler for the Crystal Barrel Collaboration, Proc. NAN'93 Conference, Moscow, 1993, Phys. At. Nuclei 57 (1994) 1693.
[22] The Obelix Collaboration, A. Bertin et al., Phys. Lett. B 408 (1997) 476.
[23] M. Foster et al., Nucl. Phys. B 6 (1968) 107.
[24] The Crystal Barrel Collaboration, A. Abele et al., Phys. Lett. B 411 (1997) 354.
[25] The ASTERIX Collaboration, B. May et al., Z. Phys. C 46 (1990) 191.
[26] J. Vandermeulen, Z. Phys. C 37 (1988) 563.
[27] The Crystal Barrel Collaboration, A. Abele et al., Phys. Lett. B 385 (1996) 425.
[28] Y. Lu, B.S. Zou, M.P. Locher, Z. Phys. A 347 (1994) 281.
[29] B.S. Zou, Proc. NAN'95 Conference, Moscow, 1995; Phys. At. Nuclei 59 (1996) 1485.
[30] D. Buzatu, F.M. Lev, Phys. Lett. B 329 (1994) 143.
[31] D. Buzatu, F.M. Lev, Phys. Lett. B 359 (1995) 393.
[32] J. Ellis et al., Phys. Lett. B 353 (1995) 319.
[33] M. Alberg, J. Ellis, D. Kharzeev, Phys. Lett. B 356 (1995) 113.
[34] The SMC Collaboration, B. Adeva et al., Phys. Lett. B 412 (1997) 414.